Proceedings World Geothermal Congress 2020+1
Reykjavik, Iceland, April - October 2021

Self-healing, Re-adhering and Carbon-steel Corrosion-mitigating Inorganic Cement Composites for Geothermal Wells at 300ºC

Tatiana Pyatina, Toshifumi Sugama

Brookhaven National Laboratory, 734 Brookhaven Ave, Upton, NY, 11973

tpyatina@bnl.gov, sugama@bnl.gov

Keywords: geothermal wells, high-temperature cements, self-healing, secondary cementitious materials, fly ash, slag, calcium-aluminate cement, acid resistance, corrosion protection, alkali activation, thermal shock

ABSTRACT

The work discusses factors affecting self-healing behavior (strength recovery and cracks' sealing), carbon steel (CS) corrosion protection and cement-steel bond-recovery, thermal shock and acid resistance of various cementitious materials under high-temperature (300°C) hydrothermal conditions. Experimental results are presented for formulations based on Ordinary Portland Cement chemistry modified with pozzolanic materials, slag, chemical and hydraulic calcium-aluminate cement-based blends and combinations of different types of fly ash at early ages (up to 28 days of the initial curing) after repeated compressive damage and short-term (5 days) exposure to the original curing conditions. Effect of environmental fluids compositions, curing conditions, physical-chemical constrains such as where the healing takes place (matrix vs. interface) on the healing process are discussed. Among the tested systems Thermal Shock Resistant Cement composed of calcium-aluminate cement, fly ash, type F, and sodium meta-silicate activator met all the target material criteria including: 1) thermal and hydrothermal stability at 300°C; 2) Compressive strength of more than 1000 psi (6.9 MPa), bond strength of 80 psi (0.55 MPa) based upon non-confined tests of sheath samples surrounding CS tube; 5) compressive strength recovery of more than 80% and bond strength recovery of more than 40% of the original strength after self-healing for 5 days under the initial curing conditions; 6) ≥30% higher sheath shear bond strength than that of OPC/SiO_2 after 6 cycles of thermal shock (one cycle, 350°C heating and 25°C water cooling by passing water through CS casing); 7) ≥30% higher lap-shear bond strength than that of OPC/SiO_2 after exposure to pH 0.2 H_2SO_4/brine for 30 days at 90°C; 8) ≥50% lower corrosion rate of CS protected by adhered and re-adhered cement to CS than that of OPC/SiO_2 after autoclaving for up to 30 days at 300°C.

ABBREVIATIONS

AAC – alkali-activated cement

CS – carbon steel

CAC – calcium-aluminate cement

CAP/CAP-A/CAP-B – calcium-aluminate phosphate cement made with CAC Secor #51 (CAP-A) or Cement Fondu (CAP-B)

EDX – energy-dispersive x-ray diffraction

FAF/FAC – fly ash, type F/fly ash, type C

GBFS – granulated blast furnace slag

IF – initial failure

MCF – micro-carbon fibers

MGF – micro-glass fibers

OPC – ordinary Portland cement

SMS – sodium meta-silicate

SHMP – sodium hexametaphosphate

TSRC – thermal shock resistant cement

YM – Young's modulus

YP – Yield point

1. INTRODUCTION

To provide durable zonal isolation, casing corrosion protection and support, geothermal wells are usually cemented from the bottom all the way up to the surface. The well-construction techniques used for geothermal wells are very similar to those of oil and gas wells and similar cement formulations are often used for well cementing. However, geothermal environments are arguably the most difficult for cements to survive (Nelson and Barlet-Gouedard 2006) because of the repeated severe mechanical and thermal stresses, highly

corrosive environments and high temperatures encountered in these wells. Commonly used well cement formulations cannot always guarantee durability of such wells. Under the stresses cement cracks, de-bonds from formation and casing compromising well integrity. Repairs of damaged underground wells are complicated, expensive and often impossible.

Cement formulations that can recover after the damage without human intervention are very attractive for such wells. Most cements have self-healing properties shortly after curing because of the presence of non-reacted cement particles that may hydrate at later times upon exposure to fluids through cracks and fractures (Huang, Ye, and Damidot 2013; Pyatina et al. 2018; Yıldırım et al. 2018). This happens because of the slow rate of hydration reactions especially at low temperatures and insufficient water content in slurries that does not allow complete cement hydration. Another way of strength recovery in cement composites is reactions of cement hydration products with environmental reactants. In construction cements this often includes carbon dioxide -cement interactions with formation of calcium carbonate in cracks and fractures that helps to recover strength and decrease permeability of cement (Jiang, Li, and Yuan 2015). Such inherent self-healing ability of cement formulations is referred to as autogenous healing. To enhance self-healing ability of cement composites slow-reacting components are deliberately added to them (Ahn and Kishi 2010; H. Huang, Ye, and Damidot 2014; Qian, Zhou, and Schlangen 2010; Şahmaran et al. 2008; Sahmaran, Yildirim, and Erdem 2013; Termkhajornkit, Nawa, and Yamashiro 2009). These latent constituents may react at later times forming binding and plugging phases, after cement hydration is completed, and environmental fluids reach them through cracks and fractures (autonomous healing).

Among the added cementitious components pozzolans are of interest because of their low cost, slow reaction under alkaline cement environments (or with added alkali activators), high-temperature stability, availability, and improved acid and thermal shock resistance of cements blended with them (Karakurt and Topçu 2011; Palomo, A. Grutzeck, M. W. Blanco 1999; T. Pyatina, Sugama, and Ronne 2016; Tatiana Pyatina 2016).

One of the important considerations for self-healing of cement composites is their toughness that controls size of the cracks formed under stress. It was shown that healing is much faster for cracks of less than 60μm in size (Li and Yang 2007; Reinhardt and Jooss 2003). Bigger fractures with smooth surfaces are more difficult to plug. Cement toughness may be improved by addition of various fibrous materials controlling cracks formation, their size and propagation.

In this work self-healing properties of three major cement systems were evaluated: 1) OPCs (Class G well cement), 2) alkali-activated cements (AACs) made with sodium-meta-silicate (SMS) as alkaline cement-forming reagent, and 3) Calcium-aluminate-phosphate (CAP) cements made with sodium-hexametaphosphate (SHMP). These cement systems were modified with natural- (SiO_2), industrial byproducts (FAF, FAC and GBFS, the last two acting as cementitious materials when combined with water), and artificial (E-type micro-glass fibers (MGF)) pozzolanic reactants. Among these pozzolanic reactants MGF was used as an additive and evaluated as a self-healing aid.

Three different AACs were tested, including: TSRC, consisting of CAC and FAF (Sugama and Pyatina 2017); FAC/FAF; and, GBFS/SiO_2 blend. All these cements were activated with SMS. Two CAP cements, containing CACs with low- and high-Fe_2O_3 contents were tested as counter reactants of SHMP (Sugama and Pyatina 2019a). These CACs were blended with FAF. To limit size of the cracks' in damaged cements, the micro-carbon fibers (MCF) were incorporated into all blends as a high-temperature reinforcement material.

2. EXPERIMENTAL PROCEDURE

Details of the experimental procedure can be found elsewhere (Sugama and Pyatina 2019b). Major oxides composition of the starting materials determined by energy -dispersive x-ray diffraction (EDX) are given in Table 1. SMS (93% purity, with the particles' size of 0.23- to 0.85-mm, trade named "MetsoBeads 2048") and SHMP were obtained from Sigma Aldrich.

Table 1. Oxide compositions of the starting materials.

Component (supplier)	Oxide composition, wt%								
	Al_2O_3	CaO	SiO_2	Fe_2O_3	Na_2O	K_2O	TiO_2	MgO	SO_3
Class G cement Dyckerhoff North Schlumberger Inc.	3.0	67.6	18.4	3.9	0.3	1.3	-	-	5.5
CAC, #80 Kerneos	75.2	24.7	-	0.1	-	-	-	-	-
CAC, #51 Kerneos	45.1	49.7	-	2.8	-	-	2.4	-	-
CAC, Fondu Kerneos	37.5-41.0	35.5-39.0	3.5-5.5	13.0-17.5	-	-	<4.0	<1.5	-
FAF Boral Material Technologies	35.0	2.7	50.1	7.1	0.30	3.1	1.6	-	-
FAC Boral Material Technologies	19.9	26.7	38.7	7.0	1.8	0.5	-	3.6	1.8
GBFS Lafarge	12.9	38.6	35.3	1.1	-	-	0.4	10.7	1.0
MGF Microglass 7280 Fibertec.	11.4	28.6	55.0	0.9	0.6	-	0.7	2.8	

All cement blends were dry blended. The OPC/SiO_2 system, contained 70wt% of class G (Dyckerhoff North) cement and 30wt% SiO_2. To prepare TSRC, the #80/FAF ratio of 60/40 by weight was used, and SMS alkali activator was added at 6% by total weight of this dry blend. The same amount of SMS also was used for two other alkali-activated cements, FAC/FAF, mixed at 60/40 mass ratio, and GBFS/SiO_2, mixed at a mass ratio of 70/30. The CAP-A or –B systems, were mixed at 60/40 CAC (#51 or Fondu respectively)/FAF ratio. These mixtures contained SHMP reactant at concentration of 6% by total weight of blend. Furthermore, 10% of MCF by total weight of dry cement blend was incorporated into all the cements tested in this work. To make slurries of appropriate similar fluidity the water/cement ratios were as follows: 0.48 for OPC (Class G) /SiO_2; 0.51 for TSRC; 0.46 for FAC/FAF; 0.45 for GBFS/SiO_2; and, 0.51 for CAP-A and –B.

After the slurries were hand-mixed, they were left at room temperature for 24 hrs. to solidify, then samples were demolded and placed into 99±1% relative humidity environment at 85ºC for 24 more hours to imitate placement into a well. Samples were further cured in non-stirred Parr Reactor 4622 filled to 20% of its volume with the test environment fluid for desired curing time at 300°C under pressure of 1200 psi (8.3 MPa). To evaluate self-healing performance of cement matrix, cylindrical cement samples (20 mm in diameter and 40 mm high) were damaged with the Instron mechanical testing system by stopping the test within no more than 40% of compressive strain after the stress-strain yield point (T. Pyatina and Sugama 2018). The cracked samples were autoclaved for 5 more days for healing (unless stated otherwise) and the stress test was repeated to determine mechanical properties after healing. For samples subjected to repeated damage the initial procedure where the testing system was stopped within no more than 40% of the yield point was repeated until the final test where the system was not stopped, and the test went to completion.

For shear-bond tests the unconfined composite sheath samples surrounding a CS tube were prepared in the following manner. The disk-shaped wooden tube-holder (49-mm-diam. by 13-mm-high) with a center hole (26- mm-diam.) was placed at the bottom of the cylindrical paper-mold of 48-mm-inner diam. and 100-mm high. The tube (125-mm-long x 25-mm-outer diam. x 3-mm-wall thickness) was inserted into the center hole of the wooden holder located at the bottom of the mold. The hand-mixed composite slurry was poured in an annular space between the tube and the mold to prepare a sheath sample (23 mm thick and 74 mm high).

The lap-shear adhesion test was conducted to determine the adhesive force of the composite coupling between CS plates according to the modified ASTM D5868 for a single-lap-joint sample. In preparing these samples, two plates, 32-mm-wide by 100-mm-long and 0.9-mm-thick each, were bonded together with the tested cement blend; the overlapped adhesive area was 1440 mm^2 (45-mm-long by 32-mm-wide). The plates with the slurry between them were cured similarly to all other cement samples at room temperature for 24 hrs., followed by 85ºC curing for 24 more hrs. and 300ºC curing for the final 24 hrs.

Each test result was the average of at least three samples. The result of the tests with cylindrical samples provided the strength recovery rate as one of the factors needed for evaluation of the self-healing performance. After the specimens were tested for strength, they were ground into very fine powder and dried at 60ºC for 24 hrs. prior to X-ray diffractometric characterization. The samples were examined using a Philips XRG 300 X-ray diffractometer with a 40 kV, 40 mA copper anode X-ray tube. The results were analyzed using the PDF-4/Minerals 2015 database of the International Center for Diffraction Data. Nikon Eclipse LV 150 3-D microscope was employed to obtain images of cracks' sealing and to explore the microstructures developed in sealed cracks. The identification of the crystalline dissolution-precipitation products in the sealed cracks was made by non-destructive Raman chemical state mapping experiments with a Renishaw® in Via™ confocal Raman microspectrometer equipped with Leica® DM2700™ upright microscope.

The blends were tested in three different environments: plain water, 0.05M sodium carbonate solution with pH 10.6 (alkali carbonate environment) and simulated geothermal brine with pH 8.1. Composition of the brine can be found in (Sugama and Pyatina 2019b). To assess the acid-resistance of the composites, the 300°C-autclaved samples were immersed in pH 0.2 H_2SO_4 solution at 90°C for up to 28 days. The volume of the acid solutions was twice as large as the volume of the samples and the solutions were replaced with fresh ones every 3 days to maintain <15% increase in pH during the treatment. After the acid exposure the specimens were rinsed with water, weighed, measured and tested for compressive strength. For the thermal shock testing, autoclaved samples were heated at 350°C for 24 hrs., and then hot samples were dipped in 25°C water immediately after removal from the oven; such heating-water quenching cycling was repeated five times. Additional thermal-shock-cycling tests were done with TSRC and OPC/SiO_2 sheath samples, cured at 300ºC then heated in an oven to 250ºC for 4 hrs. and then exposed to cold water passing through the tube at 100 ml/s for 15 minutes. The curing (300ºC)→heating (250ºC)→cold-water-through-casing cycle was repeated 20 times.

To obtain information on protection of CS by composites against brine-caused corrosion, DC electrochemical testing for the underlying CS was performed using Princeton Applied Research Model Versa STAT 4 Corrosion Measurement System. In this assessment, the CS plates, with composite-adhered and -re-adhered to its surface, were mounted into a holder, and then inserted into Ametex Model K0235 flat cell containing a 1.0 M sodium chloride electrolyte solution. The test was conducted under an aerated condition at 25°C, on an exposed surface area of 1.0 cm^2. The polarization curves were measured at a scan rate of 0.17 mVs^{-1} in the corrosion potential range from -0.4 to +0.6 V. The average corrosion rate, mm/year, associated with corrosion potential, $E_{corr.}$, and corrosion current density, $I_{corr.}$, were obtained by averaging Tafel fit results of polarization curves of three samples.

3. RESULTS AND DISCUSSION

3.1 Screening of cement composites for self-healing ability

To screen selected formulations for their self-healing ability one-day cured composites were compressively damaged and then exposed for five additional days to the original curing conditions at 300ºC for a "healing" treatment. After the healing compressive strength and Young's modulus of these composites were determined and percent of strength recovery calculated. Fractures of different nature formed in cement composites during the damage after curing in three different environments. Composites with moderate brittleness with Young's modulus between $100x10^3$ psi and $300x10^3$ psi (OPC/SiO_2 and TSRC) formed narrow, discontinuous fractures, while brittle ($300x10^3$ – $400x10^3$ psi) and very brittle (>$400x10^3$ psi) FAC/FAF and especially GBFS/SiO_2 composites formed wide, continuous cracks under the stress. For most composites the brittleness increased after curing in brine environment. Strength recovery of brittle materials was more difficult because of the nature of the fractures that they formed.

The tested composites were subjected to hot acid and thermal shock tests (see "experimental procedures" section) and their strength recovery after 5 days of the healing in the original curing environment was also evaluated. The results of all the screening tests are summarized in Table 2. The results show that most of the composites met initial mechanical-properties requirements. FAC/FAF and GBFS/SiO_2 blends, however, were too brittle, nevertheless these blends met toughness requirements. Strongly acidic environment at high temperature of 90°C was the most difficult for all the cements. Two of them (OPC/SiO_2 and GBFS/SiO_2) did not survive the 28-day long tests. Cements with high-aluminum and low calcium contents (CAP, TSRC, FAC/FAF) performed the best but their strength recovery was still below 60%. Thermal shock tests were the easiest to survive for the bulk cement samples with all the cements recovering more than 80% of their strength and TSRC, formulated specifically to withstand thermal shock stresses recovering more than 120% of the original strength. Finally, the average strength recovery, as an indicator of self-healing performance, decreased in the following order: TSRC > CAP-B> GBFS/SiO_2 and FAC/FAF >OPC/SiO_2.

Table 2. Results of screening tests for various composites based on material criteria and average compressive strength recovery in 300°C plain water, carbonate, and brine environments as well as in 90°C pH 0.2 H_2SO_4.

Composite/ Test, material criteria	Thermal and hydrothermal stability >300°C	24-hr compressive strength >1000 psi	24-hr Young's modulus (YM) <400 x 10^3 psi	Flexure toughness >0.006 $MN/m^{3/2}$	*Average strength recovery, >80%	Average strength recovery, >80% after thermal shock	Strength recovery in pH 0.2 acid at 90°C
OPC/SiO_2	Yes	Yes	Yes	Yes	C	A^+	Failed
TSRC	Yes	Yes	Yes	Yes	A	A^{++}	C
CAP-A	Yes	Yes	Yes	Yes	B	**N/A	N/A
CAP-B	Yes	Yes	Yes	Yes	B	A^+	C
FAC/FAF	Yes	Yes	No	Yes	C	A	C
GBFS/SiO_2	Yes	Yes	No	Yes	B	A^+	Failed

* A^{++} >120%, A^+ 199-100%, A >99-80%, B 79-60%, and C<60%, **Untested

3.2 Self-healing ability of repeatedly damaged composites after 1-, 5-, or 10-day initial curing

The nature of composites changes in time through continuous hydration and alkaline reactions. A composite with a structure that is ductile after the first 24 hours of curing may become brittle after extended curing exhibiting a different healing nature when damaged. Furthermore, when damaged and healed composites undergo repeated damage they may re-open original cracks, form new fractures or fail both along the original and new cracks. To evaluate a possibility of strength recovery after repeated damage and longer curing times we tested YM and compressive strength changes in composites autoclaved for up to 10 days at 300°C, repeatedly damaged and healed for 5 days after each damage under the original curing conditions (water, carbonate or geo-brine). The damage and healing were repeated 3 times.

In this work, TSRC was tested as the best candidate for self-healing, and OPC/SiO_2 was used as a reference composite. As expected, the YM value of these composites increased with the prolonged exposure in all test environments, showing that the ductile nature of composites tends to shift to brittle one after extended curing especially in carbonate and brine environments (OPC/SiO_2 blend in brine environment became brittle with YM > 300x10^3 psi after extended initial curing). Similarly, compressive strength of OPC/SiO_2, increased to >5000 psi after 10-day exposure to carbonate and brine, strongly suggesting that this composite favorably reacted with carbonate and brine chemicals. There was no significant difference in compressive strength of 5- and10-day-autocalved TSRC in these environments.

Self-healing ability of both composites persisted after the 10-day initial curing. The average strength recovery of the 2nd and 3rd time cracked TSRC in plain water was 92, 95, and 71%, respectively, for 1-, 5-, and 10-day autoclaved samples. In contrast, the recovery of OPC/SiO_2 reference composite was lower, 61, 55, and 44 % for 1-, 5-, and 10-day autoclaved samples after the repeated damage. For both composites, the recovery of 10-day autoclaved samples was nearly 25% lower than the average recovery of 1- and 5-day-autoclaved ones. The recovery was better for both composites in carbonate environment after the second-time damage and similar to that in plain water after the third-time damage (~90% for TSRC and ~60% for the OPC blend). In brine environment, for TSRC, the average recovery of compressive strength for 2nd- and 3rd time cracked composites made by 1-, 5-, and 10-day-autoclaving was 111% for the 2nd time cracked and 70% for the 3rd time cracked samples. The OPC/SiO_2 showed 47% strength recovery for the 2nd time cracked and 65% for the 3rd- time cracked samples. Table 3 shows the averaged results of the tests. As is evident, TSRC possessed great self-healing and re-self-healing properties in these three different environments after repeated damage.

Table 3. Summary compressive strength recovery rates for 2nd- and 3rd-time cracked composites averaged for composites made by 1-, 5-, and 10-day-autoclaving in plain water, carbonate, and brine at 300°C.

	Plain water		Carbonate		Brine	
	2nd crack	3rd crack	2nd crack	3rd crack	2nd crack	3rd crack
OPC/SiO_2	50 %	56 %	75 %	58 %	47 %	65 %
TSRC	83 %	89 %	91 %	88 %	111 %	70 %

3.3 Self-healing ability of composites with E-type micro-glass fiber (MGF) as healing aid

MGF is an industrial pozzolanic material that when added at 6% by weight of blend increased YM of OPC/SiO_2, CAP-A and –B, and GBFS/SiO_2 composites and did not change YM of TSRC made by 300°C-1-day-autoclaving in plain water, carbonate, and brine environments. Such YM increase made OPC/SiO_2, CAP-A and –B very brittle and further enhanced brittle nature of GBFS/SiO_2.

The average compressive strength developed by MGF-modified composites autoclaved for 24 hours in 300°C plain water, carbonate, and brine was 3640 (25.1 MPa), 2280 (15.7 MPa), 3780 (26.1 MPa), 3280 (22.6 MPa), and 7450 psi (51.4 MPa), respectively, for OPC/SiO_2, TSRC, CAP-A and –B, and GBFS/SiO_2. Table 4 gives recovery rates averaged over the three environments for the tested composites. MGF was very effective in significantly improving the recovery of two composites, TSRC and CAP-B, while some improvement also was observed for OPC/SiO_2. Increased brittleness of GBFS/SiO_2 after the addition of MGF negatively affected its recovery rates.

Increased brittleness of the blends modified with MGF in some cases caused samples failure with fragmentation under compressive damage. Since in a well cement is confined between casing and formation so the fragments may remain near the main cement body, it was of interest to see whether these fragments could re-bind during self-healing periods. For successful self-healing the fragmented sample should have appropriate chemistry and surface roughness. Ability to re-attached fragments of four composites was evaluated: TSRC as a moderately brittle composite, OPC/SiO_2 and CAP-B as brittle ones, and GBFS/SiO_2 as a very brittle one. To prepare the samples the composites were broken with excessive compressive load beyond the yield point to fragment them, the fragments were re-attached to the broken samples with a wire and the samples were re-exposed to the original curing conditions for 5 days at 300°C to evaluate a possibility of their adherence. After that the wire was removed, the samples were retested for the strength of the fragment bond (initial failure, IF) and the main sample body strength (failure at yield point, YP). Example of fragmented samples and a stress-strain curve obtained for TSRC in carbonate environment is shown in Figure 1. The point of initial failure where the re-attached fragment broke of the sample gave the compressive strength of 2000 psi (13.8 MPa) while the sample body had the strength of 2875 psi (19.8 MPa). In both cases, for the fragment bond and matrix strength the recovery was more than 100% for this composite. The only composite that did not show any fragments reattachment after repeated 5-day curing was OPC/SiO_2 blend in water environment. However, fragments of the same blend were able to re-attach to the samples in brine and carbonate environments. Similarly, CAP-A and –B, and GBFS/SiO_2 were able to re-attach the fragments in the tested environments. The best segment-bond-strength recovery and samples strength recovery in general was observed for TSRC in carbonate environment. The strength recovery of TSRC in the other two environments was also high – 115% in water and 128% in brine.

Table 4. Average strength recovery rates for composites with and without MGF.

	OPC/SiO_2	TSRC	CAP-A	CAP-B	GBFS/SiO_2
Without MGF	55%	94%	66%	62%	60%
With MGF	77%	139%	48%	117%	55%

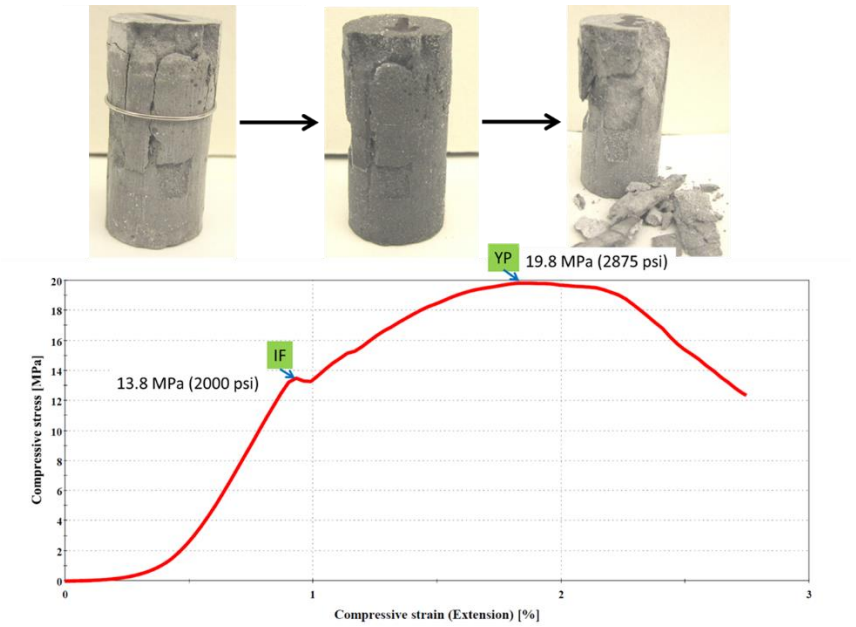

Figure 1: Compressive stress-strain curve and samples appearance before and after the healing for the fragmented TSRC in carbonate.

For GBFS/SiO_2 composite the bond-strength of attached pieces to the samples was considerably weaker than for TSRC: ~500 psi (3.4 MPa) in brine and ~700 psi (4.8 MPa) in carbonate. The initial failure for the fragmented and healed CAP-B composites showed a strong bond of 1520 psi (10.5 MPa) and the matrix strength recovery rate of 91% in brine. Nevertheless, TSRC performed the best in these reconstruction tests. The main reasons for this are its chemical nature that allowed strength increase through continuous

hydration and slow pozzolanic reactions of FAF and low brittleness of this composite that resulted in fragmentation with high contact area between the main sample body and the fragment increasing the bonding surface.

3.4 Self-healing ability of composites after long-term initial curing

3.4.1 Compressive strength recovery

Although significant stresses on geothermal-well cement may be expected after well completion, when wells are put into operation, continuous thermal and mechanical stresses can happen throughout the life of a well. On the other hand, availability of non-reacted materials for strength recovery and cracks' sealing will decrease with time limiting their self-healing ability after longer curing. To evaluate self-healing ability of the cement after longer initial curing time TSRC, as the most promising blend, and OPC/SiO_2 as a reference blend were subjected to 15- and 30-day curing before imposing initial damage followed by a 5-day healing period. MGF-modified TSRC possessed increased YM indicating increased brittleness but also showed improved strength recovery compared against non-modified TSRC. Both MGF-modified and non-modified TSRC blends were tested for self-healing after longer initial curing. Figure 2 shows strength recovery of the tested composites. The highest recovery of 117% was observed for 1-day-autoclaved TSRC/MGF composite, strongly suggesting that MGF acts as a very effective healing aid after short curing times. However, the extended curing of 15 days reduced the recovery rate to 84%, and a further reduction to 61% was observed after 30-day-curing. Non-modified TSRC did not show any significant changes in strength recovery with curing age. The recoveries ranged from 81 to 86% for 1-, 15-, and 30-day autoclaved composites. Meanwhile, the recovery of 15- and 30-day-autoclaved OPC/SiO_2 reference averaged only 37%, which was 36% lower than that of 1-day autoclaved one. Thus, it appeared that the recovery of OPC/SiO_2 reference decreased after longer curing times likely because the blend did not have any more non-reacted constituents.

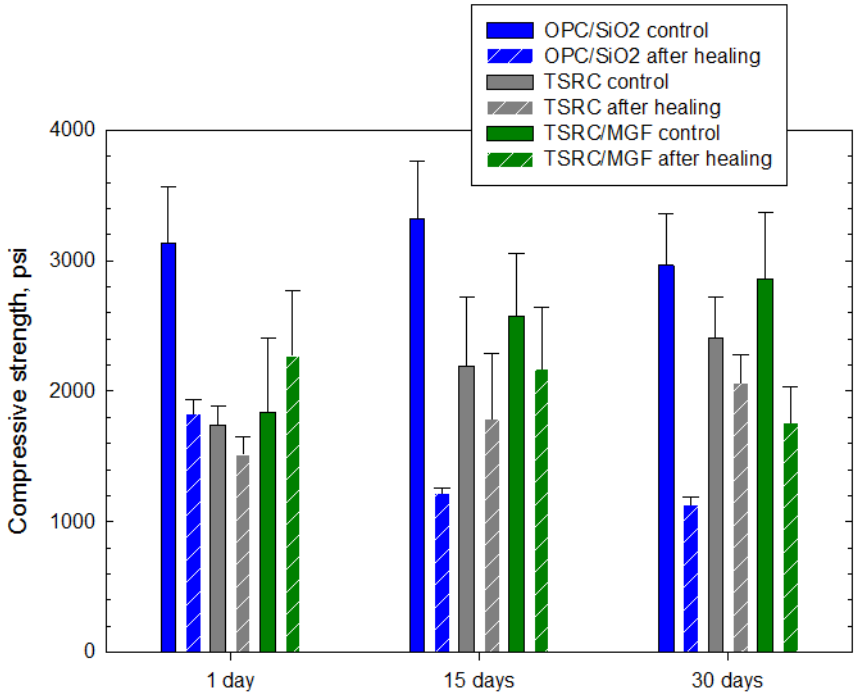

Figure 2: Compressive strength of MGF-modified TSRC, and unmodified TSRC and OPC/SiO_2 reference composites before and after 300°C-5-day-self-healing treatment.

3.4.2 Cracks sealing

Another important parameter of the self-healing process is sealing the cracks and recovering low cement permeability for corrosion protection and fluids/gas migration prevention. To evaluate sealing ability of various composites some locations on cracks of typical sizes were marked before samples' re-exposure to the curing conditions for the 5-day healing process. The depth and width of the marked areas was checked before and after the healing using 3D optical microscope. Figure 3 shows typical cracks with the width ranging from 0.1 mm to 0.2 mm for non-modified TSRC samples cured in water for 15 or 30 days before and after additional 5 days of healing. After longer curing time the availability of non-reacted blend components decreases, including non-reacted cement and FAF particles due to the continues cement hydration and FAF alkaline reactions. The lack of reactive materials may cause decreased healing and sealing ability of the composites after prolonged curing. In particular, decreased FAF content can result in decreased amounts of sealing phases such as silica and high-temperature zeolites that plug the cracks, assisting the strength recovery (Sugama and Pyatina 2019a). Additionally, water environment can provide little or none reactive ions that could help building up new phases through reactions with the cementitious composites. Moreover, longer curing times result in higher samples crystallinity and increased brittleness, promoting formation of larger cracks that are more difficult to seal.

However, moderately-sized cracks formed in TSRC and effectively sealed after only a 5-day exposure to the original curing conditions when the damage was imposed after 15- and even 30 days of the initial curing, while a 10-day treatment was required to seal a slightly wider crack >0.2 mm in a 1-day cured sample (data not shown, see (Sugama and Pyatina 2019b)). The 30-day cured sample had increased surface roughness due to the deposition of new products after the additional 5 days of healing, and the small crack was effectively sealed. The healing seemed to proceed faster for the samples with the longer initial curing before the imposed

damage. It is reasonable to rationalize that FAF reacted further after 15 and 30 days compared with that of the 1-day cured samples. In this case, the reactive ions released by the thermo-alkaline activation of FAF would be more readily available to form new phases after longer curing times. These experiments demonstrated that non-reacted FAFs remained in effect to assist the sealing activity after longer initial curing. On the other hand, the calcium-aluminate cement that reacts fast should be completely depleted by that time and is unlikely to contribute significantly to the sealing of the cracks. Furthermore, when the initial FAF source would be exhausted at longer curing time, the phase transitions and reactions of FAF-derived reaction products with the environmental ions could further assist in the cracks sealing. Consequently, if the above interpretation is valid, FAF is the major contributor to the phases that seal the cracks and the sealing will occur as along as the decomposition/reaction products of FAF are still available.

For TSRC modified with MGF the compressive strength recovery was more than 100% after the short curing-time damage but declined after longer curing times with the cement becoming more brittle. However, the cracks sealing capacity of MGF-modified TSRC was excellent after longer curing times. Figures 3 shows that both cracks formed after 15 and 30-day initial curing for modified samples were wider than for unmodified samples. The formation of these wider cracks seems to represent a brittle fracture mode. Interestingly, both cracks were sealed after the 5-day treatment, instead of the 10-day treatment required for the 1-day aged samples (data not shown). The most likely explanation for this reduced healing time is a ready availability of reactive ionic species released by the slow continuous disintegration of MGF under alkaline environment of the composite at 300°C after long-term curing. These ionic reactants released by MGF were able to form new sealing solid state phases precipitating in the cracks possibly because of the interactions with the composite components. These tests demonstrated that even after longer initial curing, TSRC samples still possessed the sealing capacity in the presence of MGF, thereby confirming MGF's role as a healing aid. Slow disintegration of MGF was important to ensure its healing aid activity after longer service time of the cementitious composite.

The excellent sealing performance of MGF-modified TSRC does not correlate with the low strength recovery of the long-term cured samples. This fact suggests that lower strength recovery was due to some other factors than cracks sealing.

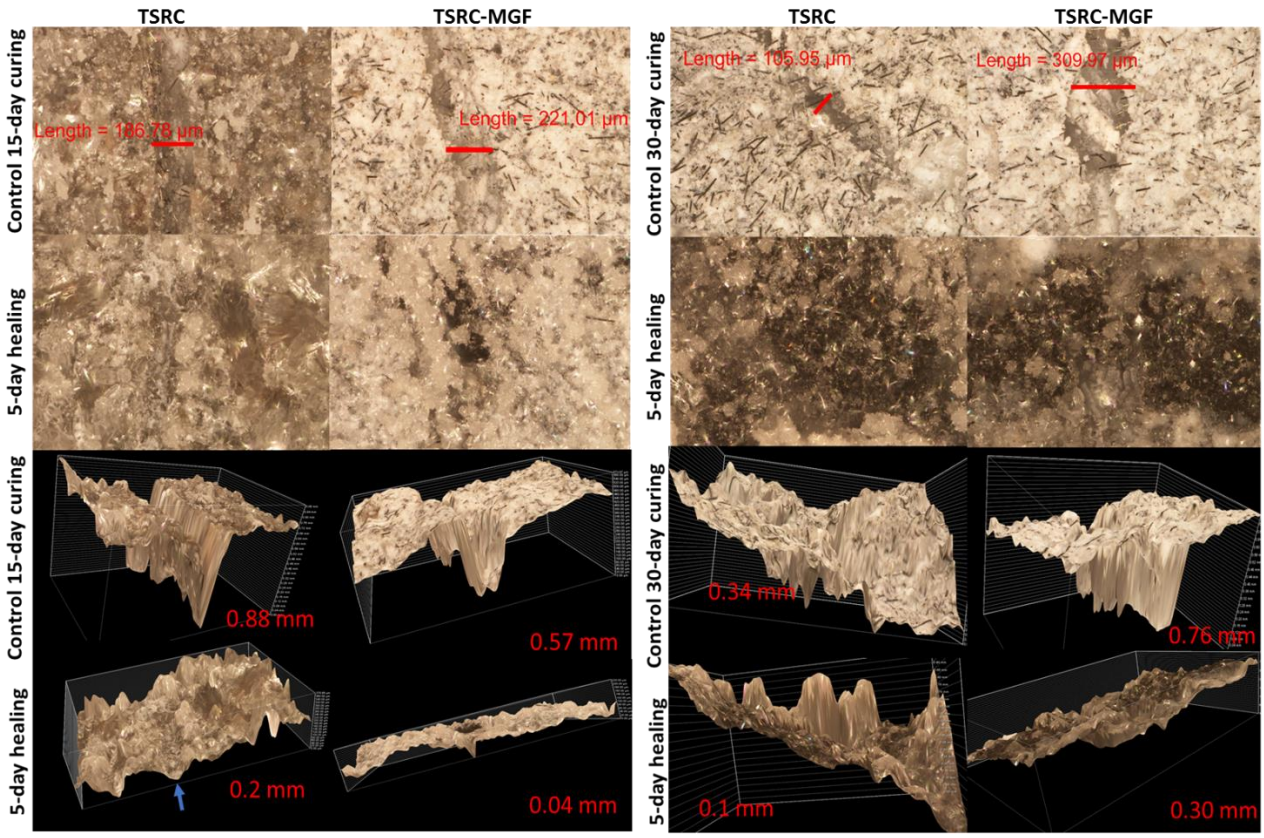

Figure 3: 15- and 30-day 300ºC cured TSRC and TSRC-MGF samples damaged and healed for another 5 days under the same conditions.

3.4.3 TSRC phase analyses and self-healing mechanism

The crystalline phases identified in non-modified TSRC samples after the first day of curing (not shown) included grossular hydroxylian, zeolite analcime, feldspar mineral dmisteinbergite, some boehmite, and non-reacted species of corundum and mullite. The patterns noticeably changed after longer curing times of 15 and 30 days. Carbonated-sodium-calcium-aluminum silicate (sodium-calcium cancrinite) replaced analcime, the peaks' intensities of dmisteinbergite, katoite and mullite decreased. Decomposition of mullite contributed to the formation of calcium-magnesium-iron-aluminum silicates (clintonite from mica group and possibly, khesinite). After the 30-day curing, aluminum in grossular was partially substituted by ferric ion to form grossular ferrian hydroxylian. Additionally, the released iron crystallized as maghemite. Decomposition of FAF also resulted in increased boehmite peaks intensities and new peaks of stishovite and quartz. A strong peak at 2Θ of 20.26, partially overlapping with the dmisteinbergite peak at 20.18 was likely from some mica-type mineral. The intensity of the peak stayed the same after the 15 and 30 days of curing. Because of the complex multi-phase composition, it was difficult to ascribe this peak to an exact phase. Several

minerals from mica group could fit the pattern including paraganite, margarite, muscovite or unnamed potassium-aluminum-magnesium-silicon oxide hydroxide. Similarly, the increased quartz signal after longer curing times complicated evaluation of the intensity of residual mullite peaks strongly overlapping with other phases and, in particular, with silica at ~2Θ of 26. In summary, at longer exposure of unmodified TSRC to high-temperature hydrothermal conditions, FAF further reacted with the release of aluminum, silicon, iron and magnesium ions that participated in phase transitions and formation of new minerals. The minerals such as iron-containing grossular further reinforced the matrix providing cement strength recovery even after long initial curing times, while the dissolution and precipitation of silica acted to seal the cracks. Some minerals participated in both strength recoveries and cracks sealing (cancrinite and boehmite). The complexity of XRD patterns did not allow a definite conclusion on whether some crystalline FAF was left after the 30 days of curing. Some peaks could be ascribed to feldspars with decreased calcium (albite, calcian) or alkali feldspars (albite, orthoclase, sanidine).

A clearly visible surface layer formed in samples cured for 15 and 30 days. It was thicker and more loosely attached to the rest of the sample after 30 days of curing than after 15 days. This stronger attachment of the surface layer to the matrix at 15 curing days likely resulted in collecting some part of the matrix with the surface samples for the XRD analyses and, at least partially, explains higher intensity of the peaks from matrix-related calcium-containing phases, such as cancrinite, khesinite, garnet (andradite) in 15-day samples than in 30-day ones.

The major crystalline surface phase was silica. High intensity of silica peaks complicated identification of other significantly smaller peaks. These were ascribed to sodium-iron-aluminum silicate or sodium-aluminum silicate, aegirine (also detected in the MGF exposed to the TSRC pore solution for 24 hrs at 300ºC); zeolites analcime and amicite; aluminum-oxide-hydroxide, boehmite and mica-type mineral, paragonite with limited certainty. Likewise, some peaks could be from feldspars with decreased calcium (albite, calcian) or alkali feldspars (albite, orthoclase, sanidine). These minerals crystallized after most calcium from CAC already reacted and only FAF participated in the formation of new phases.

MGF-modified TSRC cured in water had higher peak intensities of analcime, katoite and grossular. Some quartz and some iron-containing calcium-silicate phase – srebrodolskite formed in these samples after the first day of curing at 300ºC. A peak at 26.4 (found only in the pattern of glass-modified samples) is likely from keatite SiO_2. Presence of mica type mineral, paragonite, iron-containing grossular was possible. The samples with MGF were richer in silica already after the first curing day.

Comparison of 15- and 30-day cured modified TSRC clearly demonstrates that MGF stabilize analcime. Because of analcime stabilization there is less cancrinite obtained through analcime→ cancrinite transition. There are higher intensity peaks of iron-containing grossular (andradite), iron-magnesium silicate, khesinite and iron oxide. Among the three reaction products, iron-containing grossular, iron-magnesium silicate and analcime, formed in samples of modified TSRC, the first two products enhanced the strength recovery and analcime participated in cracks' sealing.

Some mica-type mineral was the same as for the samples without MGF. The mica minerals that fit the pattern included: paraganite-2M1 (01-083-2128); celadonite/muscovite 3T (04-021-4959); margarite 2M1 (04-013-3004) or potassium-aluminum-magnesium-iron silicate oxide hydroxide (01-079-6488(6487)). Similarly, some peaks could be ascribed to feldspars with decreased calcium (albite, calcian) or alkali feldspars (albite, orthoclase, sanidine). Additionally, presence of magnesium-containing mineral, polymorph of serpentine, lizardite, was possible in MGF-modified samples. Small amounts of magnesium could be coming from the reacting glass fibers. Magnesium minerals, in this case lizardite and khesinite, increase the strength of the cement matrix. High-temperature calcium silicate wollastonite formed only in glass-modified samples likely from silicon and calcium released by decomposing MGF.

Like for TSRC samples, silica dominated XRD patterns of surface samples of TSRC-modified with MGF. Other possible phases included cancrinite, sodium-aluminum silicate, aegirine and feldspars with reduced calcium as in the case of the reference TSRC samples.

To compliment XRD phase identification Raman analyses of cracks areas were conducted on samples exposed to steam conditions for healing after the imposed compressive damage. These analyses allowed targeting specific locations on a sample. Crystalline phases gave clear signals, while signals from amorphous phases were more spread and often luminescent. Additionally, similar to the XRD patterns, presence of many different phases complicated the spectra and phase identification. Nevertheless, some phases, found in large quantities in crack areas were clearly identifiable for both MGF-modified and unmodified samples. Figure 4a shows a Raman spectrum of a crack area for a 15-day cured TSRC sample. The pattern unambiguously represents crystalline silica, that was a major phase filling the cracks after 15 and 30 days of curing for both control and modified samples. In addition to silica and in agreement with the XRD results Raman showed spectra corresponding to iron-containing mineral aegirine, that appears in the spectra after longer curing times when fly ash reactions proceed to release iron (Figure 4b). Two more phases unmistakably present in the spectra of the filled-crack areas included bohmite and analcime. Both could be found in the samples even after short curing time of the first 5 days of cracks healing. However, for the most part, silica spectrum dominated the spectra of the crack areas or complex overlapping spectra of many phases were obtained for the samples (Figure 5). Relatively broad peaks with shoulders indicated multiple phases contributing to the signal. In addition to earlier mentioned silica, bohmite, albite and high-temperature zeolite (amicite, in this case), the spectrum could be formed by feldspar minerals with varying calcium and potassium contents. The presence of feldspars is likely since albite matched a spectrum at another location and XRD patterns suggested possibility of these minerals in TSRC samples. Changes in calcium content after long curing times may be explained by increased contribution of silicon, aluminum and alkali metals by fly ash and glass fibers participating in high-temperature reactions.

Raman results confirmed XRD findings on surface composition of crack sealing phases in TSRC samples that for the most part included silica, high-temperature zeolites (analcime and amicite), sodium-iron-silicate (aegirine), aluminum oxide hydroxide (bohmite) and feldspar minerals with varied calcium and alkali metals content.

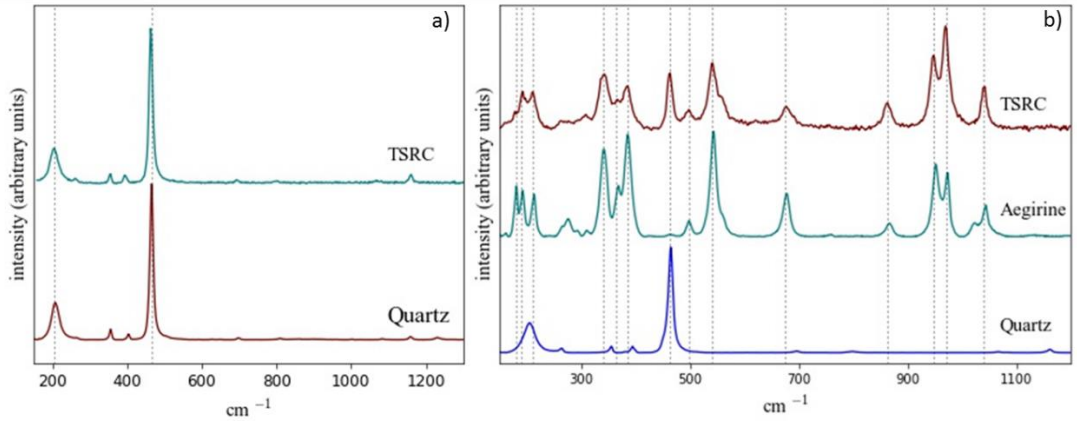

Figure 4: Raman spectrum of MGF-modified TSRC sample after 15 days of curing at 300ºC in water environment and patterns of quartz and aegirine corresponding to the spectrum.

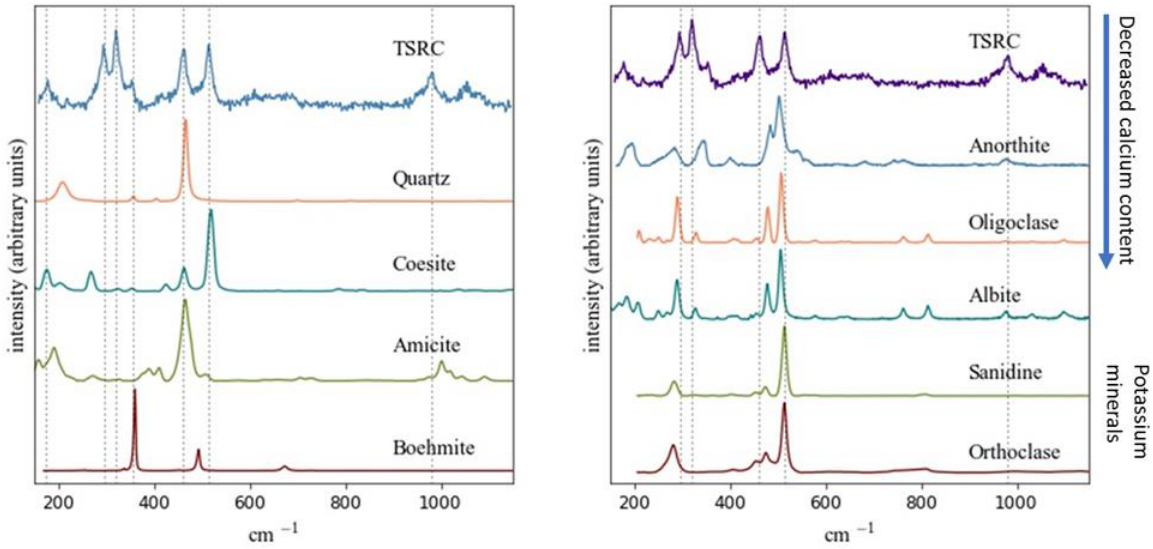

Figure 5: Raman spectrum of TSRC-MGF sample after 30 days of curing at 300ºC in water environment and reference patterns matching the spectrum.

Based on the XRD test results, Figure 6 depicts a schematic of possible crystalline phase transitions in the matrix of TSRC samples cured at 300ºC for different periods.

In TSRC the first forming phases, crystallizing shortly after the cement set are, for the most part, hydration and SMS-reaction products of CAC. They include hydrogrossular, feldspars (dmisteinbergite and anorthite) and boehmite. At longer exposure times garnets (various stoichiometries of hydrogrossular) become predominant. Continuous slow reactions of FAF introduce additional aluminum, silicon, iron and magnesium into the crystalline phases. Garnets with higher silicon content and with aluminum partially substituted by iron replace earlier formed grossular. Boehmite and silica contents noticeably increase. Additionally, mica group calcium-magnesium and calcium-magnesium-iron silicates form in the matrix. The slow reactions of FAF contributing such crystals-building ions as aluminum, silicon, iron and magnesium result in the recoveries of compressive strength for damaged samples. MGF become an additional source of silica, aluminum, calcium, and some magnesium and iron. These ions stabilize analcime for longer time, preventing its conversion into cancrinite and improving cracks sealing. Additional silica from MGF crystalizes in the fractures further filling them. MGF decomposition in alkali cement environments also introduces ions that form magnesium and iron-containing phases increasing strength of the matrix. MGF reacts slowly, and its effect becomes more noticeable after longer curing times in samples exposed to 300ºC for 15 or 30 days.

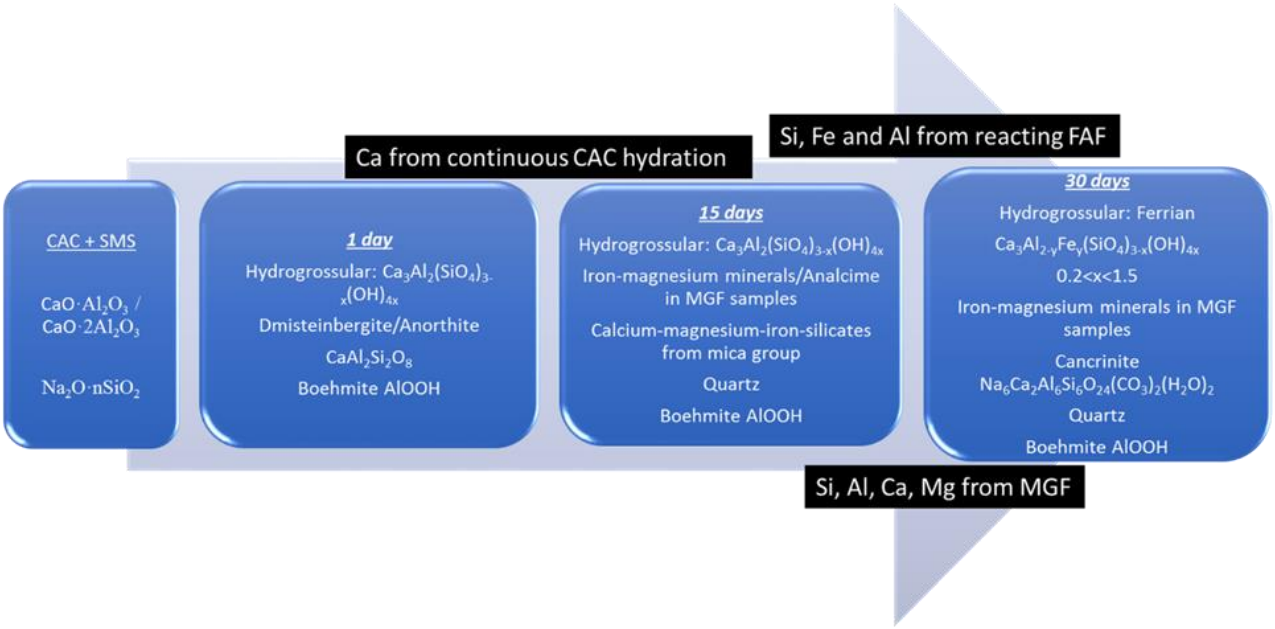

Figure 6: Crystalline phases formation and transitions for TSRC samples cured in water environment at 300ºC.

Based on the information obtained by XRD and Raman tests, Figure 7 proposes phase transitions occurring at the surface and in the fractures of TSRC samples as the curing progresses. The major crystalline phases participating in cracks' sealing from early curing times are zeolite analcime and silica mostly from sodium silicate and calcium aluminate cement early reactions. As the curing continues analcime converts to cancrinite through carbonation, so the content of analcime declines. Another zeolite, sodalite, forms and more silica precipitates because of alkali dissolution of fly ash and MGF (for MGF-modified samples) with release of silicon and aluminum ions. Silica remains the main sealing phase throughout the healing, and especially after longer curing times when FAF and MGF dissolution releases more of silicon ions. In addition to silicon, alkali dissolution of FAF and MGF contributes more aluminum, some iron and alkalis to the pool of reacting ions after longer curing. They form (sodium, potassium, calcium)-aluminum-silicates from feldspar group of minerals with varied calcium and alkali metal contents replacing originally formed calcium-aluminum silicate feldspars, anorthite and dmisteinbergite. Sodium iron silicate, aegirine, also precipitates in the cracks.

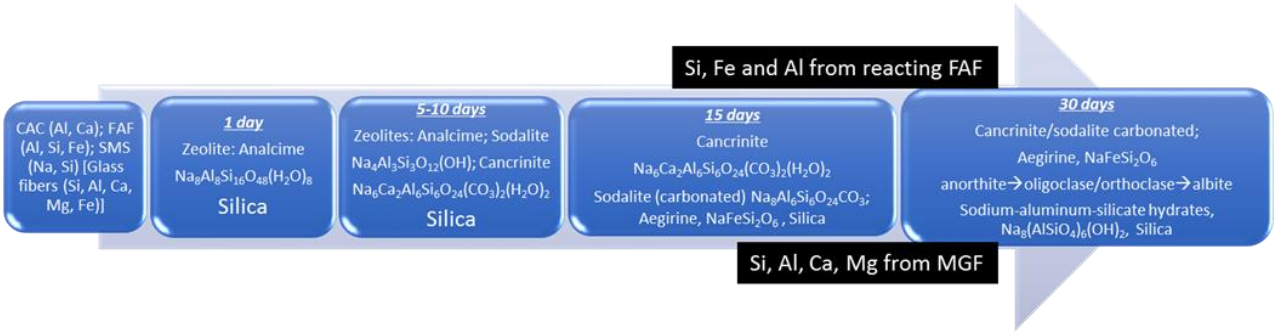

Figure 7: Crystalline phases formation and transitions at the surface and in the cracks of TSRC samples cured in water environment at 300ºC.

3.5 Corrosion protection and re-adhering behavior of debonded composite sheath to CS casing surface

One of the main cement functions in subterranean wells is casing corrosion protection. Corrosion is a common problem in aggressive environments of geothermal wells where casing metal is subjected to repeated chemical, thermal, mechanical stresses. Casing corrosion takes place when cement is permeable for corrosive electrolytes or/and cement-casing bond is broken and an annulus forms along the casing allowing migration of corrosive fluids and gasses. Figure 8 compares performance of OPC/SiO_2 and TSRC composites in repeated severe thermal shock (TS) cycles in plain water. In these tests, each cycle consisted of curing sheath samples at 300ºC for a day then heating them up to 250ºC for 4 hours followed by cold water flow through the casing (100 ml/s) for 15 minutes and then re-exposing the samples to the 300ºC autoclave for another day. This cycling was repeated 20 times.

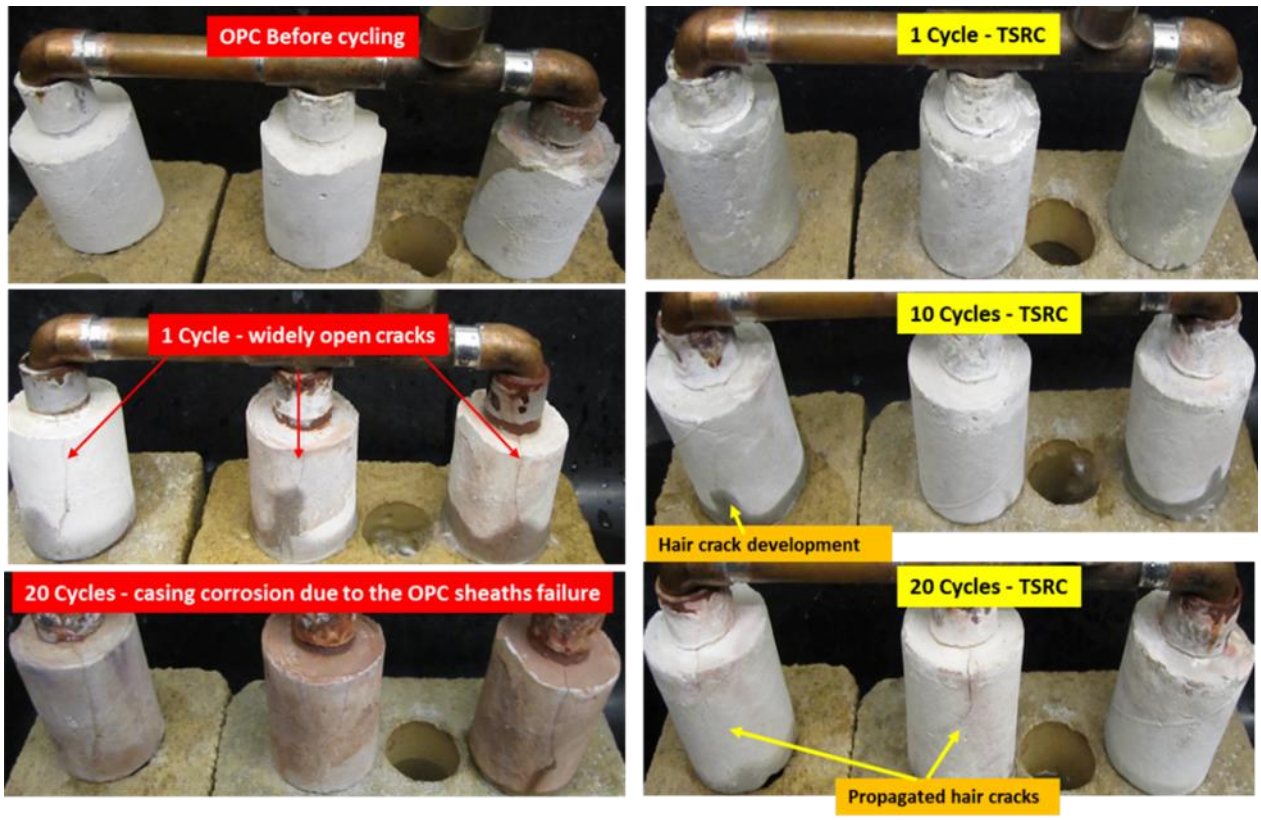

Figure 8: Changes in the appearance of OPC/SiO_2 (left) and TSRC (right) sheath samples during the severe cycling (one cycle: 250ºC dry heat → cold water through the casing → 300ºC hydrothermal curing).

Such severe TS conditions resulted in cement sheath cracking during the first flow of the cold water for OPC/SiO_2 blend with formation of wide cracks going throughout the cement sheath. Broken cement-casing bond caused water contact with the steel tube and severe metal corrosion (Figure 9 top). Even more severe corrosion problems may be expected in geo-brines. TSRC blend, on the other hand, cracked after the 10th cycle, developing thin, non-continuous cracks resulting in some corrosion spots on the metal after 20 cycles. However, significant part of the casing was still covered by cement and protected from corrosion after 20 cycles (Figure 9 bottom).

Figure 9: Appearance of OPC/SiO_2 sheath samples (top) and TSRC sheath samples (bottom) after 20 severe TS cycles.

There is a high probability of casing-cement bond failure under conditions of geothermal wells, so there is an obvious interest in a possibility of cement re-adherence to the metal. Results of re-adherence experiments (300ºC) for OPC/SiO_2 and TSRC non-modified and MGF-modified blends are given in Figure 10. All tests were done in plain water. In general, due to the different nature of the materials bond recovery is not as easy as strength recovery for cement composites. All 30-day-autoclaved composites demonstrated

increased bond strength, compared with 1-day-autoclaved ones. The value of 30-day sheath-shear bond strength was 70 psi (0.48 MPa) for OPC/SiO_2, 82 psi (0.57 MPa) for TSRC, and 245 psi (1.69 MPa) for TSRC/MGF, which is tantamount to 2.1-, 1.1-, and 1.3-fold rise in bond strength, respectively, over the 1-day bond strength. As expected, for strongly-bonded TSRC/MGF composite, the excessive sheath shear bond strength caused the development of undesirable multi-radial cracks in the sheath during the debonding test (Figure 10 right). As a result, the bond strength recovery for this sample was only 28%. Overall, MGF-free TSRC exhibited the best bond recovery performance of 49% and 57% for 1-day- and 30-day-autoclaved composites respectively. The bond recovery of the 30-day autoclaved OPC/SiO_2 was 38%.

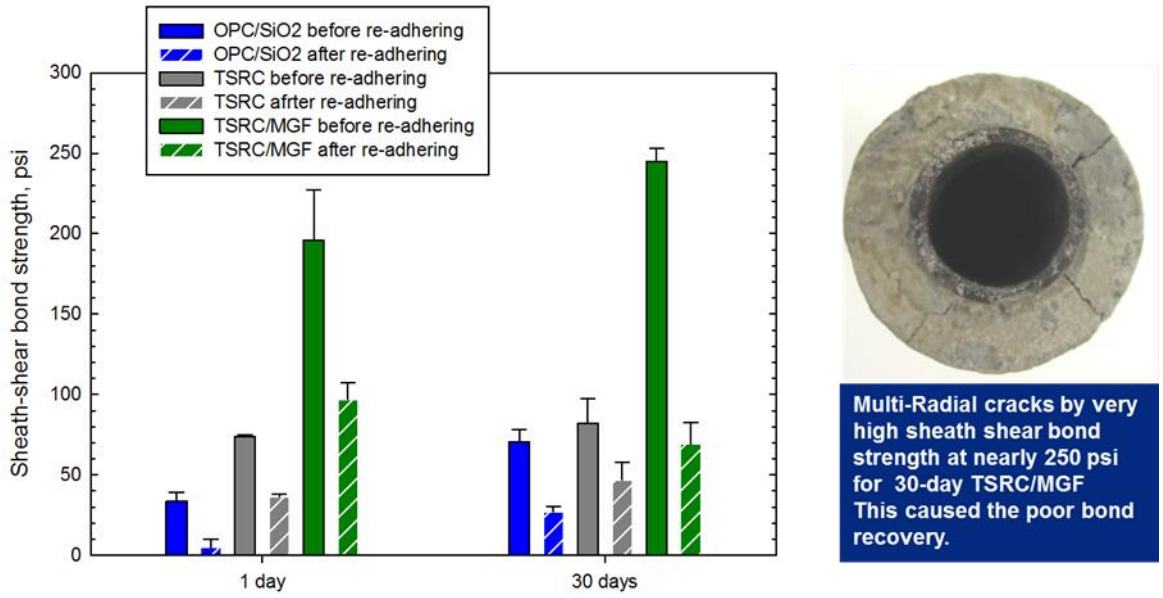

Figure 10: Sheath-shear bond strength of 1- and 30-day-acutoclaved TSRC/MGF composite sheath, and MGF-free TSRC and OPC/SiO_2 sheaths before and after the re-adherence treatment in 300°-plain water for 5 days.

Another important parameter of cement sheath performance, carbon steel corrosion protection by cement, was investigated with the use of lap-shear bond samples (Figure 11). After debonding of the composite sheath from CS the remaining composite layer must protect CS from corrosion and this protection must improve after the re-adherence treatment. To evaluate whether this was the case the CS plate/cement/CS plate lap joint samples were prepared by autoclaving them in 24-hrs-300°C plain water. In this work, OPC/SiO_2 and TSRC modified and unmodified with MGF were tested, and their ability to inhibit corrosion of CS was evaluated for composite layer adhering to CS surfaces after the 1st and 2nd lap-shear bond tests by DC electrochemical polarization in brine. The details of preparation for the 2nd bond strength test can be found in (Sugama and Pyatina 2019b). After the 1st bond strength test, two debonded CS plates were reattached by steel wire (Figure 11), and then autoclaved for 5 additional days in plain water at 300°C. After this re-adherence treatment the wire was removed and the 2nd time bond strength test was conducted and the plate with the thinner composite layer was further tested to obtain quantitative corrosion-related data showing whether the re-adherence treatment improved corrosion protection of CS. The data included the corrosion rate of CS (from electrochemical measurements at 3 different locations) and thickness of the composite remaining on CS after the bond tests.

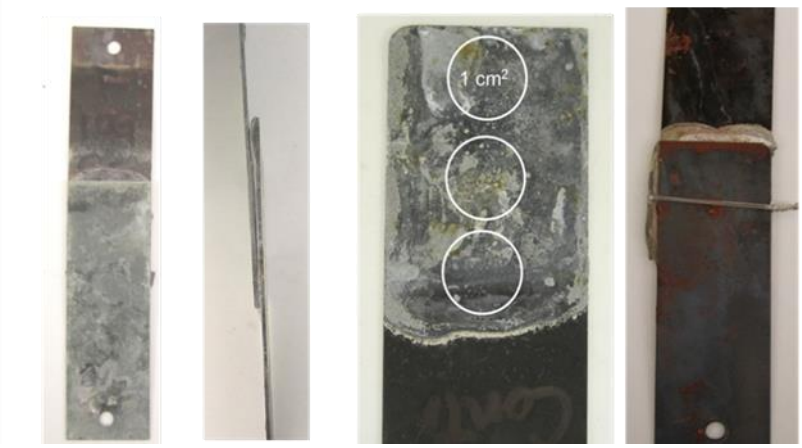

Figure 11: Lap-shear bond samples (from left to right): sample appearance before the 1st lap-shear bond tests, three locations of electrochemical corrosion testing, sample with the metal plates re-attached by wire after lap-shear bond tests before a repeated exposure.

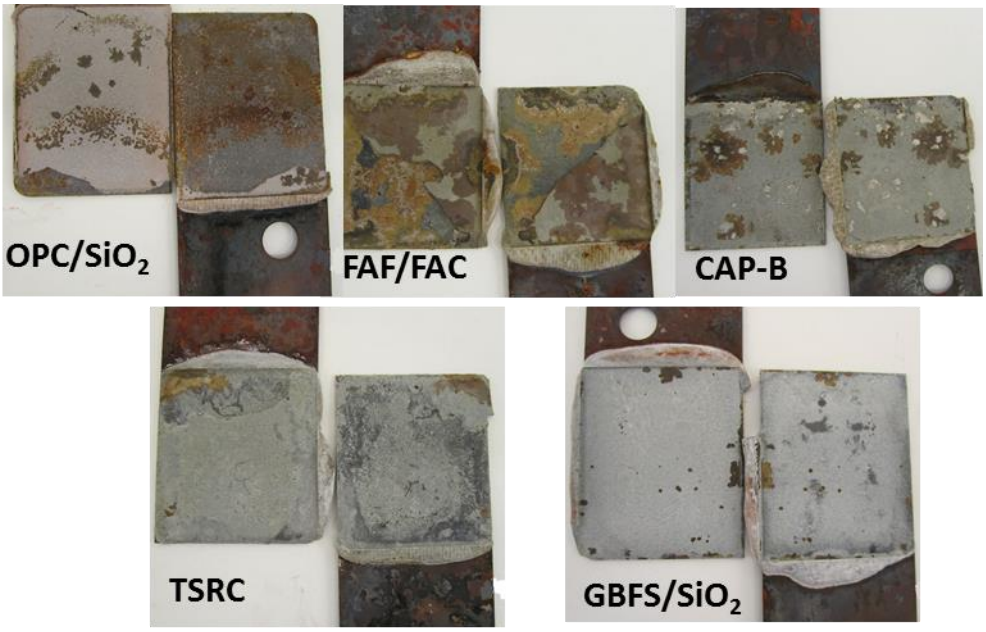

Figure 12: Appearance of OPC/SiO_2, FAF/FAC, CAP-B, TSRC, and GBFS/SiO_2 1-day 300ºC-cured plates after the bond-strength test.

The lap-shear bond samples were visually examined after the bond-strength test to identify the failure mode: cohesive failure in composite layer, adhesive failure at interfaces between composite and CS or a mixed cohesive-adhesive failure. Figure 12 shows appearance of plates with five composites. The OPC/SiO_2 composite failed adhesively at the interfacial region between the composite and CS. This happened because of the poor bonding between the composite and the steel causing local corrosion stains. FAF/FAC and CAP-B composites also showed local corrosion stains. In the case of FAF/FAC the corrosion may be a result of porous microstructure that the composite formed at the interface, due to the slow alkaline and hydration reactions of this blend, allowing fluids penetration to the CS surface. As for CAP-B composite, its slurry has a low pH value (8.5-9 vs. 12-13 for OPC and alkali-activated blends) that does not allow formation of a protective layer at the interface and, as a result, is less favorable for corrosion prevention. TSRC and GBFS/SiO_2 blends failed cohesively with composite layer still protecting plates from corrosion after the failure. Further experiments focused on MGF-modified and non-modified TSRC blend and OPC/SiO_2 used as a reference. The lap-shear bond strengths of these blends after 1- and 30-day curing are given in Figure 13. The strength increased after the longer curing for OPC/SiO_2 and especially for the TSRC-MGF blends. The bond-strength of non-modified TSRC did not change significantly suggesting relatively fast formation of the interfacial phases providing the bonding in the case of TSRC, while slower reacting glass fibers contributed to the bond strength after longer curing.

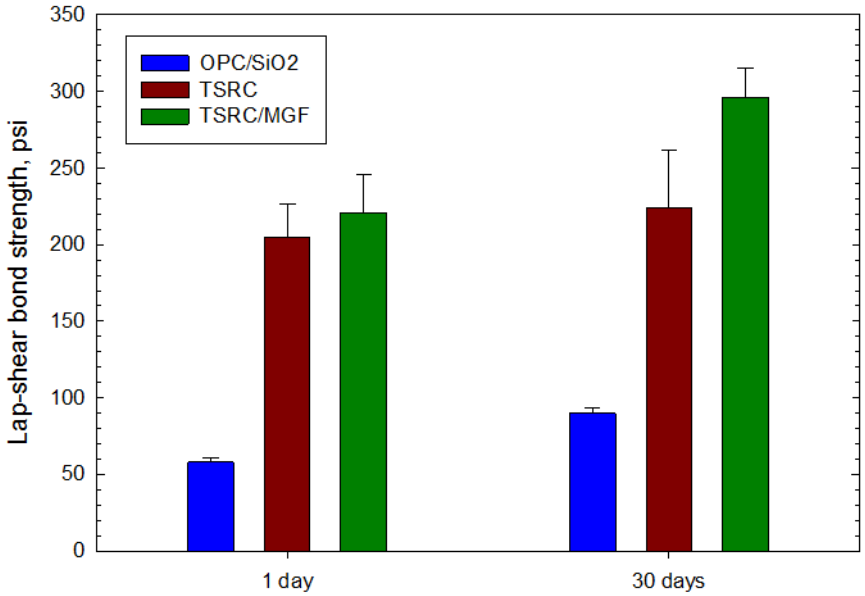

Figure 13: Lap-shear bond strength of MGF-modified and nonmodified OPC/SiO_2 and TSRC after 1- and 30-day 300ºC-curing.

After the first lap-shear-bond tests the thickness of the composite's layers covering the plates decreased in the order: OPC/SiO_2-MGF (0.128 mm) > TSRC-MGF (0.117 mm) > TSRC (0.10 mm) > OPC/SiO_2 (0.076 mm). The corrosion rate decreased in the order:

OPC/SiO_2 (0.68 mm/year) > TSRC (0.36 mm/year)>OPC/SiO_2–MGF (0.32 mm/year)>TSRC-MGF (0.18 mm/year). MGF fibers clearly improved corrosion protection performance of the composites, especially in the case of the OPC/SiO_2 blend.

After the re-adherence treatment the protective layer thickness of both modified and non-modified TSRC samples increased by nearly 2.3 times. The thickness of OPC/SiO_2- modified and non-modified with MGF did not change significantly. Nevertheless, the corrosion rate of re-adhered OPC/SiO_2-covered plate decreased, likely because of the cement layer densification resulting in decreased permeability. The corrosion rate also decreased for TSRC composites. The corrosion rate of the re-adhered CS plates covered with various composites decreased in the following order: OPC/SiO_2 (0.49 mm/year) > OPC/SiO_2-MGF (0.23 mm/year) ~TSRC (0.23 mm/year) > TSRC-MGF (0.16 mm/year).

The protective layer thickness and corrosion rate for OPC/SiO_2 and TSRC modified and non-modified with MGF after 1- and 30-day initial curing is shown in Figure 14. The protective layer thickness increased 2.4 times for the 30-day cured samples in comparison with the 1-day cured samples for both TSRC and OPC/SiO_2 composites. However, in the case of Portland cement blend the steel corrosion product, magnetite, formed sports on the metal surface indicating progressing corrosion while TSRC samples had composite coverage on both plates after the bond test (cohesive failure). The increased thickness of the cement over the steel plates resulted in reduced corrosion rates after the 30-day treatment. The corrosion rate of the 30-day autoclaved samples dropped from 0.18 to 0.16 mm/year for TSRC/MGF, from 0.36 to 0.25 mm/year for non-modified TSRC and from 0.68 to 0.59 mm/year for OPC/SiO_2.

After the re-adherence treatment, the thickness of re-adhered 30-day-autocalved TSRC/MGF and TSRC composites over CS, somewhat increased to 0.32 mm from 0.28 mm and to 0.25 mm from 0.23 mm, respectively, decreasing corrosion rate to 0.13 mm/year for TSRC/MGF and 0.2 mm/year for TSRC, underscoring that although the interfacial debondement for 30-day-aged TSRC/MGF and TSRC composites occurred, the composites remaining on the CS surface provided an excellent corrosion protection of CS against brine-caused corrosion. By contrast, the OPC/SiO_2 layer thickness did not change after re-adherence treatment and the corrosion rate increased from 0.59 to 0.64 mm/year.

For good corrosion protection of CS two factors were very important: good wetting and spreading of composite slurries over CS surfaces providing uniform coverage by the composite layer and good adhesive behavior of composite to CS, allowing developing of strong interfacial bond between the composite and CS. The tests demonstrated that alkali-activated TSRC/MGF blend showed the best wetting and adhesive behaviors, while performance of non-activated OPC/SiO_2 blend was relatively poor.

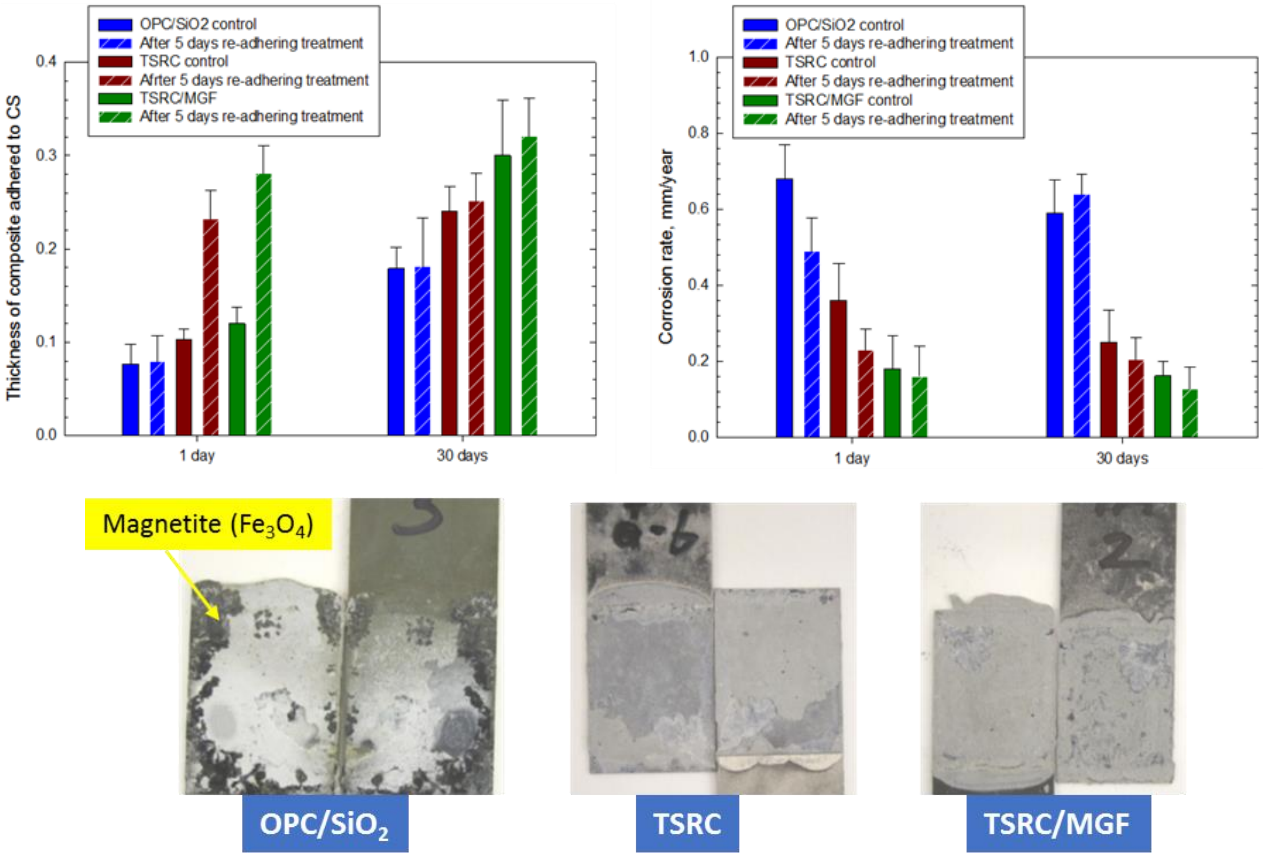

Figure 14: Thickness of composite adhesive layer at CS surfaces, corrosion rate of underlaying CS, and appearance of debonded CS plates for 300°C-30-day-autoclaved MGF-modified and non-modified TSRC and OPC/SiO_2 composites.

4. CONCLUSIONS

Self-healing properties (strength recoveries and cracks' sealing) of various cementitious composites were investigated in water, alkali carbonate and geothermal brine at 300°C. Additionally, effects of acid environment (pH 0.2, 90°C, H_2SO_4) and thermal shock (350°C dry) on composites strength recoveries were studied to identify the best self-healing cements for geothermal applications. The tested

composites included OPC/SiO_2 blends as reference, TSRC, FAC/FAF, GBFS/SiO_2, CAP (with different calcium-aluminate cements). Among the tested composites FAC/FAF blends showed a brittle nature after a 1-day curing in water and carbonate, while GBFS/SiO_2 became very brittle in all curing environments. Brittle FAC/FAF blend formed wide difficult-to-seal fractures and a very-brittle blend of GBFS/SiO_2 fragmented under compressive stress. TSRC was moderately brittle after a day curing at 300ºC forming narrow cracks. Only TSRC met material criterion of strength recovery, recovering more than 80% of its strength after 5 days of healing under the original curing conditions. Acid tests presented the most severe conditions for strength recovery where OPC/SiO_2 and GBFS/SiO_2 blends expanded and failed after 14 days and the rest of the tested composites eroded but recovered some strength (all less than 60%). All composites performed well under conditions of moderate thermal shock (24 hours at 350ºC dry heat) recovering more than 80% of the strength when cured for additional 5 days after the thermal shock tests. On the other hand, all composite lost some bond strength because of thermal shock (250ºC heat), TSRC bond strength decrease was the smallest (21%), the strength loss varied between 33 and 40% for other composites.

TSRC was further tested for its ability to recover strength after repeated damage. The composite was able to recover >85% of its strength in different environments for the 2nd and 3rd time cracked samples cured for 1 or 5 days before the first damage. The 3rd time cracked composite cured for 10 days before the first damage recovered 78% of its strength. The average recovery rate for TSRC cracked 3 times and cured for 1-, 5-, or 10 days before the first damage was 87%, which was 50% higher than the recovery of OPC/SiO_2 composite. Alkali carbonate environment was the most favorable for both strength recovery and cracks sealing.

To further improve self-healing performance slow-reacting E-type glass fibers were added to selected blends as a healing aid. Except for TSRC, addition of MGF increased composites' brittleness. Nevertheless, MGF-modified TSRC, CAP-B and OPC/SiO_2 composites increased their recovery rates to 139%, 117% and 77% respectively. In the case of CAP-A and GBFS/SiO_2 the recovery rate reduced. MGF-modified composites were tested for their ability to re-bind fragments for samples subjected to extensive compressive load resulting in their fragmentation. The broken samples of all composites were successfully re-bonded to the original samples after exposure of 5 days in plain water, carbonate, and brine environments at 300ºC. The bond strength of the re-bonded fragment was determined from the point of initial failure on strain-stress curve. In some cases (e.g. TSRC in water and brine) there was no initial failure point on the strain-stress curve when samples failed forming new cracks. TSRC/MGF outperformed all other tested composites, recovering more than 100% of the strength in all environments: 120% in water, 150% in carbonate and 128% in brine.

Phase analyses of TSRC matrix and fractures showed that different phases participate in the composite strength recovery and cracks sealing. The strength building phases included feldspar minerals (dmisteinbergite, anorthite), aluminum oxide hydroxide (boehmite, tohdite), garnet (hydrogrossular). After longer curing times calcium was partially and later completely replaced by sodium in feldspar minerals that may be explained by increased contribution of silicon, aluminum and alkali metals from fly ash and glass fibers participating in high-temperature reactions. The de-calcification was especially important in alkali carbonate environment.

Crystalline phases that sealed the fractures precipitated from the pore solution and included for the most part silica and zeolite, analcime or amicite. Aluminum oxides hydroxides contributed to the sealing as well. The crack-sealing phases mostly came from slow dissolution and reactions of FAF and MGF (for MGF-modified slurries). Under alkaline carbonate environment precipitation of both silica and analcime was the most significant causing the fastest sealing of the cracks. After longer curing times, both in water and carbonate, analcime converted to carbonate mineral, feldspathoid, cancrinite. Addition of MGF stabilized analcime likely through slow glass disintegration with release of the reactive ions participating in reactions with the composites counterions. Brine environment was not favorable for formation of sealing phases. Magnesium-containing minerals assisted in strength recovery but did not seal the cracks.

TSRC evaluated for composite-steel bond recovery also outperformed two other tested blends OPC/SiO_2 and CAP-B. Its bond recovery rate after 5 days of healing at 300ºC was 49% compared to 15% for OPC/SiO_2 and 26% for CAP-B. The re-adhering ability of TSRC was preserved in samples cured for 30 days before the initial bond damage. Thirty-day cured TSRC recovered 57% of the bond strength. The bond strength nearly tripled for TSRC modified with MGF. However, such strong bond resulted in radial cracks during the damage and lowered bond recovery (28%). Importantly, for TSRC protected steel samples, bonds failed cohesively (in the cement layer) so that a cement layer remaining on metal surface still protected it from corrosion. The corrosion rate of CS protected by TSRC was 0.36 mm/year (vs. 0.68 for OPC/SiO_2), it further decreased when TSRC was modified with MGF (0.18 mm/year) and for samples cured for 30-days (0.2 mm/year non-modified TSRC and 0.13 mm/year for MGF-modified TSRC).

In summary, TSRC outperformed all other tested composites in all the conducted evaluations demonstrating the best self-healing, self-re-adhering abilities, corrosion protection, acid and thermal shock resistance under simulated conditions of high-temperature geothermal wells.

ACKNOWLEDGEMENTS

This publication was based on the work supported by the Geothermal Technologies Office in the US Department of Energy (DOE) Office of Energy Efficiency and Renewable Energy (EERE), under the auspices of the US DOE, Washington, DC, under contract No. DE-AC02-98CH 10886. Raman data were acquired in SoMAS' Nano-Raman Molecular Imaging Laboratory (NARMIL), a community facility dedicated to environmental sciences' applications and founded with NSF-MRI grant OCE-1336724.

REFERENCES

Ahn, T-H., and T. Kishi. 2010. "Crack Self-Healing Behavior of Cementitious Composites Incorporating Various Mineral Admixtures." *Journal of Advanced Concrete Technology* 8: 171–86.

Farage, M.C.R., J. Sercombe, and C. Gallé. 2003. "Rehydration and Microstructure of Cement Paste after Heating at Temperatures up to 300 °C." *Cement and Concrete Research* 33(7): 1047–56.

Huang, H., G. Ye, and D. Damidot. 2014. "Effect of Blast Furnace Slag on Self-Healing of Microcracks in Cementitious Materials."

Cement and Concrete Research 60: 68–82.

Huang, H., G. Ye, and D. Damidot. 2013. “Characterization and Quantification of Self-Healing Behaviors of Microcracks Due to Further Hydration in Cement Paste.” *Cement and Concrete Research*.

Jiang, Z., W. Li, and Z. Yuan. 2015. “Influence of Mineral Additives and Environmental Conditions on the Self-Healing Capabilities of Cementitious Materials.” *Cement and Concrete Composites* 57.

Karakurt, C., and I.B. Topçu. 2011. “Effect of Blended Cements Produced with Natural Zeolite and Industrial By-Products on Alkali-Silica Reaction and Sulfate Resistance of Concrete.” *Construction and Building Materials* 25(4): 1789–95.

Li, V.C., and E.H. Yang. 2007. “Self-Healing in Concrete Materials in Self Healing Materials: An Alternative Approach to 20 Centuries of Materials Science.” In *Springer Series in Materials Science*, eds. R. Hull, R.M.Jr. Osgood, J. Parisi, and H. Warlimont. , 161–93.

Nelson, E.B., and V. Barlet-Gouedard. 2006. “Thermal Cements.” In *Well Cementing*, eds. E.B. Nelson and D. Guillot. Sugar Land, Texas: Schlumberger, 319–39.

Palomo, A., M.W. Grutzeck, and M.T. Blanco. 1999. “Alkali Activated Fly Ashes: A Cement for Future.” *Cement and Concrete research* 29(May 2014): 1323–29.

Pyatina, T., and T. Sugama. 2018. “Cements for High-Temperature Geothermal Wells.” In *Cement Based Materials*, eds. H. Saleh and R.O. Abdel Rahman. London, 221–35.

Pyatina, T., T. Sugama, and A. Ronne. 2016. “Self-Repairing Geothermal Well Cement Composites.” In *Transactions - Geothermal Resources Council,*.

Pyatina, T., T. Sugama, A. Ronne, and G. Trabits. 2018. “Self-Repairing Properties of OPC Clinker/Natural Zeolite Blend in Water and Alkali Carbonate Environments at 270°C.” *Advances in Cement Research* 30(1).

Pyatina, Tatiana. 2016. “Resistance of Fly Ash – Portland Cement Blends to Thermal Shock.” 28(2): 121–31.

Qian, S.Z, J . Zhou, and E. Schlangen. 2010. “Influence of Curing Condition and Pre-Cracking Time on the Self-Healing Behavior of Engineered Cementitious Composites.” *Cement & Concrete Composite* 32: 686–93.

Reinhardt, H-W., and M. Jooss. 2003. “Permeability and Self-Healing of Cracked Concrete as a Function of Temperature and Crack Width.” *Cement & Concrete Research* 33: 981–85.

Şahmaran, M.G., G Yildirim, and T.K. Erdem. 2013. “Self-Healing Capability of Cementitious Composites Incorporating Different Supplementary Cementitious Materials.” *Cement & Concrete Composites* 35: 89–101.

Şahmaran, M.G., S. B. Keskin, G. Ozerkan, and I. O. Yaman. 2008. “Self-Healing of Mechanically-Loaded Self Consolidating Concretes with High Volumes of Fly Ash.” *Cement and Concrete Composites* 30(10): 872–79.

Sugama, T., and T. Pyatina. 2017. *Alkali-Activated Cement Composites for High Temperature Geothermal Wells*. Scientific Research Publishing, Inc.

Sugama, T., and T. Pyatina. 2019a. “Self-Healing, Re-Adhering, and Carbon-Steel Corrosion Mitigating Properties of Fly Ash-Containing Calcium Aluminum Phosphate Cement Composite at 300 °C Hydrothermal Temperature” *Cement & Concrete Composite* 99: 1–16.

Sugama, T, and T. Pyatina. 2019b. “Self-Healing , Re-Adhering , and Corrosion-Mitigating Inorganic Cement Composites for Geothermal Wells at 270-300C.” *BNL-211405-2019-INRE* (February).

Termkhajornkit, P., T. Nawa, and Y. Yamashiro. 2009. “Self-Healing Ability of Fly Ash-Cement Systems.” *Cement & Concrete Composites* 31(195–203).

Yıldırım, G., A.H. Khiavi, S. Yeşilmen, and M.G. Şahmaran. 2018. “Self-Healing Performance of Aged Cementitious Composites.” *Cement and Concrete Composites* 87.